J. Phase Equilib. Diffus. (2019) 40:820–829
https://doi.org/10.1007/s11669-019-00772-6

Experimental Investigation of Diagram Equilibria in the Co-Nb-Re Ternary System

Xingjun Liu[1,2,3] · Dan Wu[1] · Lingling Li[1] · Mujin Yang[1] · Jinbin Zhang[1] · Jiahua Zhu[1] · Yuechao Chen[1] · Shuiyuan Yang[1] · Jiajia Han[1] · Yong Lu[1] · Cuiping Wang[1]

Submitted: 18 June 2019 / in revised form: 12 November 2019 / Published online: 25 November 2019

Abstract In this study, the isothermal sections of the Co-Nb-Re ternary system at 1200, and 1300 °C have been experimentally determined combining the means of electron probe microanalysis (EPMA) and x-ray diffraction (XRD). The obtained experimental results showed that: (1) The Laves phase of λ_3-Co_2Nb (C36) was stable at 1300 °C. The temperature was beyond its stability limit in Co-Nb binary system. (2) The solubility of Re in the λ_3 phase was so large that the nearest λ_2-Co_2Nb (C15) phase was essentially surrounded. (3) The solubility of Re in the μ-Co_7Nb_6 phase was 34.0 at.% at 1200 °C and 35.2 at.% at 1300 °C, respectively. (4) The liquid phase existed at 1300 °C dissolving about 4.0 at.% Re, but it was absent at 1200 °C. (5) The solid solution phase of (εCo, Re) extended from Re-rich to Co-rich side.

Keywords Co-Nb-Re ternary system · electron microprobe · high-temperature alloys · phase equilibria

✉ Cuiping Wang
wangcp@xmu.edu.cn

[1] College of Materials and Fujian Provincial Key Laboratory of Materials Genome, Xiamen University, Xiamen 361005, People's Republic of China

[2] State Key Laboratory of Advanced Welding and Joining, Harbin Institute of Technology, Harbin 150001, People's Republic of China

[3] Institute of Materials Genome and Big Data, Harbin Institute of Technology, Shenzhen 518055, People's Republic of China

1 Introduction

Co-based superalloys that have better resistance of oxidation and hot corrosion than Ni-based superalloys are regarded as competitive high-temperature materials.[1,2] In order to obtain better high temperature performances to meet the increasing requirements of the aerospace field, One of the most effective methods to improve the elevated temperature property is adding refractory elements such as Mo, Re, Nb, W, Ta.[3-12] For example, the melting point of elemental Re (rhenium) is 3186 °C. As an additive element, elemental Re can not only improve the strength and creep resistance of Co-based superalloys, but also refine the morphology of the alloys.[6-9] Doping refractory element of Nb can improve high-temperature strength, creep resistance, oxidation resistance and corrosion resistance.[10-12] However, in Co-based superalloys, the brittle and detrimental TCP (topologically close packed) phases easily form under high temperature and pressure if the element additions are excessive. Therefore, the amounts of the Re and Nb are under precise control and the knowledge of phase equilibria in the Co-Nb-Re system is needed. However, the experimental information and phase diagram of this ternary system are not established. Hence, investigating the phase equilibria of Co-Nb-Re system is necessary.

The three binary systems of Co-Nb, Co-Re and Nb-Re constitute Co-Nb-Re ternary system, as shown in Fig. 1. For the Co-Re binary system, it was ever published by Elliott.[13] Later, Predel[14] also reported the results for the Co-Re binary system. In 2014, Liu et al.[5] estimated the Co-Re system and the phase equilibria were consistent with the experimental data. Recently, Guo et al.[15] reassessed the Co-Re system with the new thermodynamic parameters of pure Re. The newly assessed Co-Re phase diagram by Guo et al.[15] was applied in this work. The Co-Re

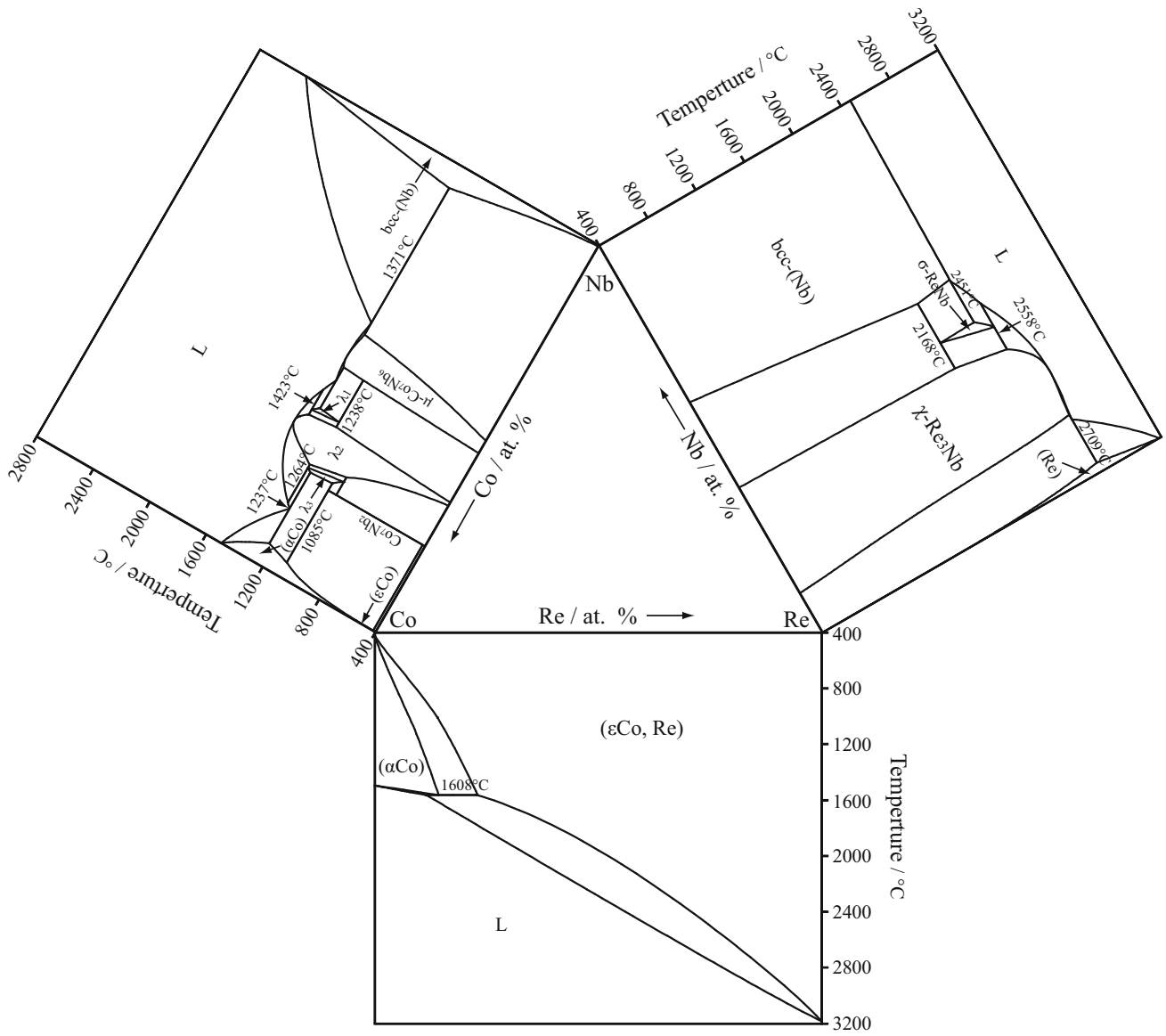

Fig. 1 Binary phase diagrams constituting the Co-Nb-Re ternary system[15,21,26]

system[15] is simple because there are only two solid phases of (αCo) and (εCo, Re) and no intermediate phases. The (εCo, Re) phase has a wide homogeneity range. A peritectic reaction of L + (εCo, Re) ↔ (αCo) exists in the Co-Re system.

Pargeter and Hume-Rothery[16] investigated the equilibrium diagram of the Co-Nb system by a combination of thermal analysis, microscopical metallography, and x-ray diffraction techniques. They reported there were only three intermetallic compounds of Laves phase λ_2, λ_3 and μ-Co_7Nb_6 in the system. Later, Bataleva et al.[17] firstly found five intermetallic compounds existing in the Co-Nb binary system. Kumar[18] thermodynamically evaluated the system using the data from Bataleva et al.[17] They described the λ_1 and λ_3 Laves phases as stoichiometric phases $Co_{16}Nb_9$ and Co_3Nb. In 2008, Stein et al.[19] reinvestigated the Co-Nb system and determined the existence of the five phases of μ-Co_7Nb_6, Co_7Nb_2, λ_3, λ_2, and λ_1. He et al.[20] reassessed the binary system using a two-sublattice model $(Co, Nb)_2(Co, Nb)$ for the λ_1 and λ_3 phases. Later, He et al.[21] re-adjusted the thermodynamic parameters and re-described the Co-Nb system. This work adopted the Co-Nb phase diagram evaluated by He et al.[21] The Co-Nb system is a special system where the Laves phases λ_1, λ_2, and λ_3 with different structure types (hexagonal, cubic and hexagonal) occur as stable phases. There are the other two intermediate compounds of μ-Co_7Nb_6 and Co_7Nb_2. The λ_1 phase is stable in the temperature range from 1238 to 1423 °C. The eutectoid reaction: $\lambda_1 \leftrightarrow \lambda_2$ + μ-Co_7Nb_6 occurs at 1238 °C where the λ_1 phase decomposes. The

composition range of the λ_1 phase is small. Similarly, the λ_3 exists in the temperature range from 1029 to 1264 °C. It disappears at 1029 °C as it changes into the λ_2 phase and Co_7Nb_2 phase from the eutectoid reaction: $\lambda_3 \leftrightarrow \lambda_2 + Co_7Nb_2$.

The Nb-Re binary system has been investigated by many researchers.[22-26] Greenfield and Beck[22] confirmed the existence of the χ phase. Steadman and Nuttall[23] determined the site occupancies in the χ phase using x-ray diffractions. Knapton[24] ever determined the invariant reactions and the congruent melting of the χ phase by alloyage and confirmed two eutectic points at 2673 K, 53% Re (L ↔ bcc + σ) and 3003 K, 88% Re (L ↔ χ + hcp), respectively. In addition, a peritectic point was found at 2723 K and 57% Re (L + χ ↔ σ), the congruent melting of the χ phase was 3073 K. Savitskii et al.[25] reported a peritectic reaction (L + hcp ↔ χ) existing at 2793 K and a eutectic reaction (L ↔ bcc + χ) existing at 2613 K. Liu et al.[26] conducted a thermodynamic description of the Nb-Re binary system via the CALPHAD method using present first-principles calculations. The Nb-Re binary system assessed by Liu et al.[26] is adopted in this work. There are two solid phases of bcc-(Nb) and (Re), two intermetallic phases of σ-ReNb and χ-Re_3Nb in the Nb-Re phase diagram. The σ-ReNb phase forms from the peritectic reaction of L + χ-Re_3Nb ↔ σ-ReNb and occupies a composition range from 57.1% Re at 2168 °C to 60.0% Re at 2558 °C. The χ-Re_3Nb phase occupies a large composition range. Table 1 summarizes all the solid phases and intermediate phases in three binary systems.

This work intends to experimentally determine the phase equilibria relationship of Co-Nb-Re ternary system at 1200 and 1300 °C by means of electron probe microanalysis, x-ray diffraction.

2 Experimental Procedure

From the pure metals of cobalt (99.9 wt.%), niobium (99.9 wt.%) and rhenium (99.9 wt.%), All 27 alloys were prepared in the form of atomic ratios (at.%) and measured with a semi-micro analytical balance with an accuracy of at least 0.5 mg. The bulk alloys with nominal compositions were prepared by the arc smelting using a non-consumable tungsten electron in the atmosphere of argon. The ingots were remelted for at least five times to promote complete mixing and melting, thus to obtain the homogeneous ingots. Subsequently, the samples were cut into pieces by wire-cutting machine.

The samples were wrapped with niobium foils and encased in quartz tube, which were evacuated and back-filled with pure argon gas several times. The titanium scrap was put in the quartz tube to prevent oxidation, similarly. Afterwards, the samples were annealed at 1200 and 1300 °C. The time of heat treatment varied from 15 to 50 days according to the temperature and compositions. The alloys containing more than 20 at.% Re were heat-treated for a longer time. After the heat treatment, the samples were quenched in ice water, then grinded with sandpaper and polished using diamond paste.

The microstructure of the heat-treated alloys were characterized by EPMA (JXA-8100R, JEOL, Tokyo, Japan). The voltage was 20 kV and the current was 1.0×10^{-8} A. Pure metals of Co, Nb and Re were used as standards. The powder x-ray diffraction (XRD) measurements was carried out on a Philips Panalytical X-pert diffractometer (Bruker Daltonic Inc., Billerica, MA, USA) with Cu Kα radiation at 40 kV and 40 mA to analyze the crystal structure of the alloys. The scanning range of 2θ was from 20° to 90° at a step size of 0.0167°.

Table 1 Crystal structures of each phase in the Co-Nb-Re ternary system

System	Phase	Pearson's symbol	Space group	Prototype	Strukturbe Type	Reference
Re-Nb	(Re)	*hP*2	*P*6$_3$/*mmc*	Mg	*A*3	15
	χ-Re_3Nb	*cI*58	*I*-43*m*	αMn	*A*12	15
	σ-ReNb	*tP*30	*P*4$_2$/*mnm*	σCrFe	$D8_b$	15
	bcc-(Nb)	*cI*2	*Im*-3*m*	W	*A*2	15
Co-Re	(αCo)	*cF*4	*Fm*-3*m*	Cu	*A*1	21
	(εCo, Re)	*hP*2	*P*6$_3$/*mmc*	Mg	*A*3	21
Co-Nb	(αCo)	*cF*4	*Fm*-3*m*	Cu	*A*1	26
	(εCo)	*hP*2	*P*6$_3$/*mmc*	Mg	*A*3	26
	λ_3-Co_2Nb	*hP*24	*P*6$_3$/*mmc*	Ni_2Mg	*C*36	26
	λ_2-Co_2Nb	*cF*24	*Fd*-3*m*	Cu_2Mg	*C*15	26
	λ_1-Co_2Nb	*hP*12	*P*6$_3$/*mmc*	Zn_2Mg	*C*14	26
	μ-Co_7Nb_6	*hR*39	*R*-3*m*	Fe_7W_6	$D8_5$	26
	bcc-(Nb)	*cI*2	*Im*-3*m*	W	*A*2	26
	Co_7Nb_2	*mC18*	*C*2/*m*	Zn_2Ni_7	…	26

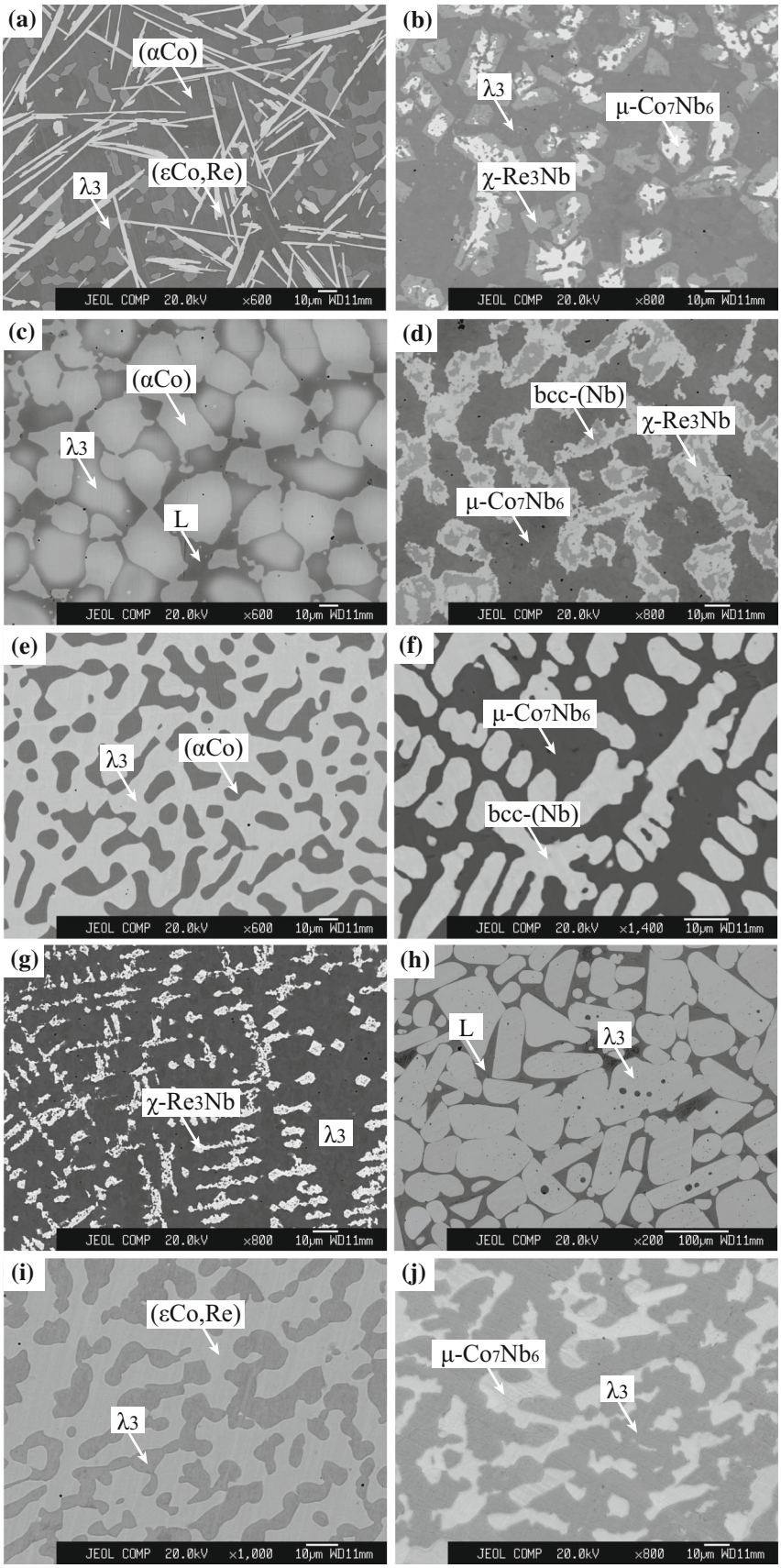

Fig. 2 BSE images of the typical ternary Co-Nb-Re alloys: (a) The $Co_{79}Nb_6Re_{15}$ alloy annealed at 1200 °C for 35 days; (b) the $Co_{35}Nb_{30}Re_{35}$ alloy annealed at 1200 °C for 50 days; (c) the $Co_{76}Nb_{13}Re_{11}$ alloy annealed at 1300 °C for 15 days; (d) the $Co_{25}Nb_{40}Re_{35}$ alloy annealed at 1300 °C for 25 days; (e) the $Co_{72}Nb_{18}Re_{10}$ alloy annealed at 1200 °C for 35 days; (f) the $Co_{23}Nb_{58}Re_{19}$ alloy annealed at 1200 °C for 35 days; (g) the $Co_{44}Nb_{25}Re_{31}$ alloy annealed at 1200 °C for 50 days; (h) the $Co_{76}Nb_{20}Re_4$ alloy annealed at 1300 °C for 15 days; (i) the $Co_{71}Nb_{12}Re_{17}$ alloy annealed at 1300 °C for 15 days; (j) the $Co_{59}Nb_{40}Re_1$ alloy annealed at 1300 °C for 15 days

3 Results and Discussion

3.1 Microstructure

Figure 2 shows the typical back-scattered electron (BSE) images of ternary Co-Nb-Re alloys annealed at 1200 and 1300 °C with different compositions. The three-equilibrium microstructures are shown in Fig. 2(a), (b), (c) and (d) and the two-equilibrium microstructures are shown in Fig. 2(e), (f), (g), (h), (i) and (j). Figure 3 shows the corresponding x-ray diffraction results. In the following paper, the liquid phase is denoted as L.

The BSE image of $Co_{79}Nb_6Re_{15}$ alloy annealed at 1200 °C for 35 days was shown in Fig. 2(a). It was a three-phase equilibrium of the (εCo, Re), (αCo) and λ_3 phases. The white strip phase was (εCo, Re), grey phase was λ_3 and black phase was (αCo). Figure 2(b) shows the white μ-Co_7Nb_6 phase, light grey χ-Re_3Nb phase and dark grey λ_3 phase existing in an equilibrium in the $Co_{35}Nb_{30}Re_{35}$ alloy annealed at 1200 °C for 50 days. The corresponding XRD pattern was presented in Fig. 3(a). The characteristic peak clearly verified the three-phase microstructure. For the $Co_{76}Nb_{13}Re_{11}$ alloy, the L phase, (αCo) phase and λ_3 phase were observed after annealing at 1300 °C for 15 days. Figure 2(d) shows the BSE image of the white χ-Re_3Nb phase, grey bcc-(Nb) phase and black μ-Co_7Nb_6 phase in the $Co_{25}Nb_{40}Re_{35}$ alloy annealed at 1300 °C for 25 days. Figure 3(b) shows the corresponding XRD pattern, and the phases of χ-Re_3Nb, bcc-(Nb) and μ-Co_7Nb_6 were clearly distinguished by the different symbols. In the $Co_{72}Nb_{18}Re_{10}$ alloy (1200 °C for 35 days), the black (αCo) phase and white λ_3 phase were found, as shown in Fig. 2(e). The (αCo) phase was evenly distributed in the matrix λ_3 phase. Figure 2(f) is the BSE images of $Co_{23}Nb_{58}Re_{19}$ alloys annealed at 1200 °C for 35 days. Two phases of μ-Co_7Nb_6 and bcc-(Nb) existed in an equilibrium. The white phase was bcc-(Nb) and black phase was μ-Co_7Nb_6. The XRD analysis of the $Co_{23}Nb_{58}Re_{19}$ alloy is presented in Fig. 3(c), which is consistent with the result in Fig. 2(f). Figure 2(g) shows a two-phase equilibrium of χ-Re_3Nb (white phase) and λ_3 (grey phase) in the $Co_{44}Nb_{25}Re_{31}$ alloy annealed at 1200 °C for 50 days. The $Co_{76}Nb_{20}Re_4$ alloy annealed at 1300 °C for 15 days contained two phases of λ_3 and L in Fig. 2(h). The λ_3 phase dissolved in the L phase. The two-phase microstructure of the dark grey λ_3 phase and light grey (εCo, Re) phase was identified in the $Co_{71}Nb_{12}Re_{17}$ alloy annealed at 1300 °C for 15 days, as shown in Fig. 2(i). The BSE image of $Co_{59}Nb_{40}Re_1$ alloy quenched from 1300 °C was showed in Fig. 2(j). The white phase of μ-Co_7Nb_6 and grey phase of λ_3 were

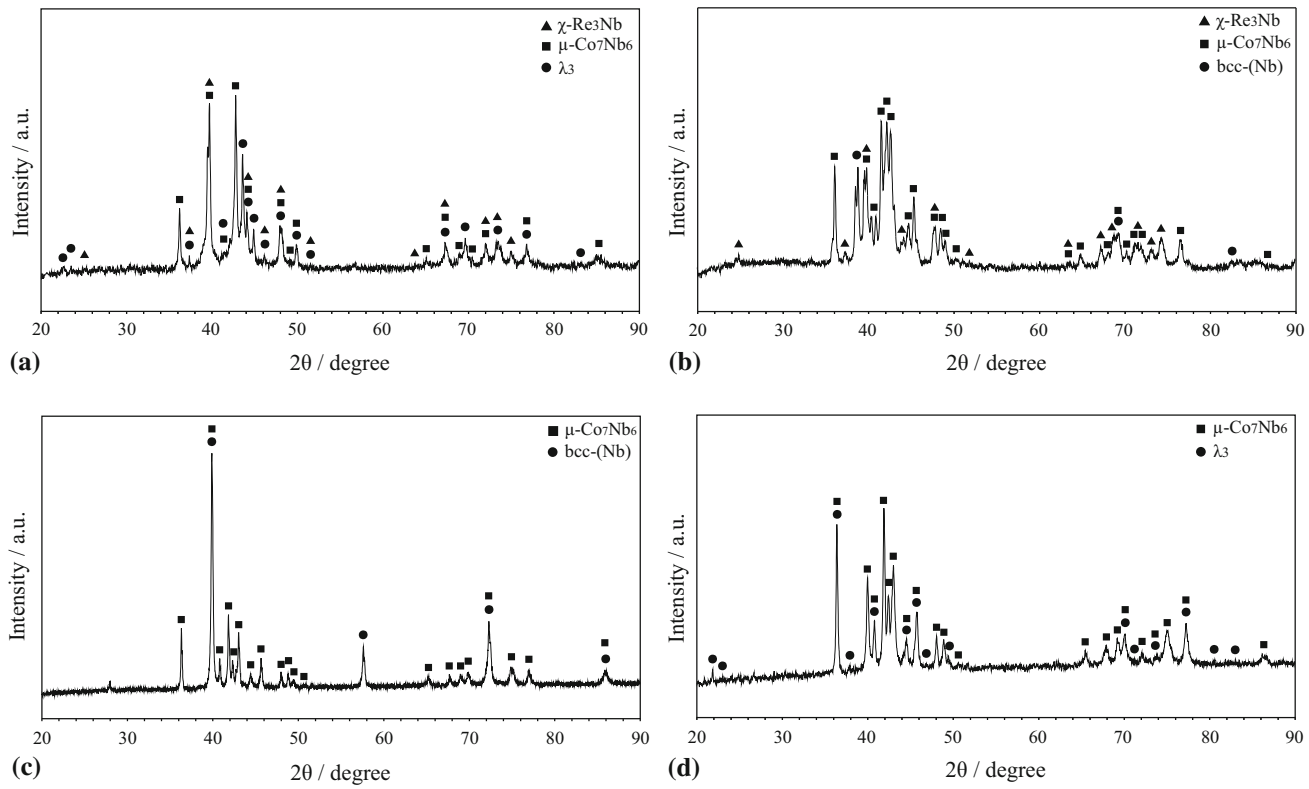

Fig. 3 X-ray diffraction patterns obtained from: (a) the $Co_{35}Nb_{30}Re_{35}$ alloy annealed at 1200 °C for 50 days; (b) the $Co_{25}Nb_{40}Re_{35}$ alloy annealed at 1300 °C for 25 days; (c) the $Co_{23}Nb_{58}Re_{19}$ alloy annealed at 1200 °C for 35 days; (d) the $Co_{59}Nb_{40}Re_1$ alloy annealed at 1300 °C for 15 days

observed in an equilibrium and their structures were confirmed by XRD pattern in Fig. 3(d).

3.2 Isothermal Sections

Tables 2 and 3 present the equilibrium compositions of the Co-Nb-Re ternary system at 1200 and 1300 °C, respectively. The phase relationships at the isothermal sections of 1200 and 1300 °C are determined according to the experimental data, as shown in Fig. 4(a) and (b). Different symbols are used to characterize λ_2-single phase, λ_3 single phase, two-phase equilibrium, and three-phase equilibrium. The determined three-phase equilibria are presented by the solid triangles while the undetermined three-phase equilibria are presented by the dashed triangles.

The 1200 °C isothermal section of Co-Nb-Re ternary system is shown in Fig. 4(a). Four intermetallic compounds of λ_2, λ_3, μ-Co_7Nb_6 and χ-Re_3Nb, three solid solution phases of (εCo, Re), (αCo) and bcc-(Nb) were found in this isothermal section. Four alloys ($Co_{48}Nb_{33}Re_{19}$, $Co_{64}Nb_{25}Re_{11}$, $Co_{63}Nb_{23}Re_{14}$, $Co_{60}Nb_{35}Re_5$) were confirmed to be λ_3 single phase and two alloys ($Co_{66}Nb_{29}Re_5$, $Co_{69}Nb_{29}Re_2$) were λ_2 single phase. The λ_3 phase dissolved a large solubility of Re (21.7 at.%) and wrapped around the λ_2 phase from the left side to the right side. The solubility of Re in the λ_2 phase was about 4.8 at.%. The solubility of Re in μ-Co_7Nb_6 reached up to about 34.0 at.%. The solubility of Co in the χ-Re_3Nb phase was measured to be approximately 18.0 at.%. The composition range of the (εCo, Re) phase was wide, extending from Re-rich side to Co-rich side. The (εCo, Re) phase dissolved about 18.9 at.% Nb. There were five three-phase regions of (εCo, Re) + (αCo) + λ_3, λ_3 + (εCo, Re) + χ-Re_3Nb, λ_3 + μ-Co_7Nb_6 + χ-Re_3Nb, μ-Co_7Nb_6 + χ-Re_3Nb + bcc-(Nb),

Table 2 Equilibrium compositions of the Co-Nb-Re ternary system at 1200 °C determined in the present work

Temperature, °C	Alloy, at.%	Annealed time, days	Phase equilibria	Composition, at.%					
			Phase 1/Phase 2/Phase 3	Phase 1		Phase 2		Phase 3	
				Nb	Re	Nb	Re	Nb	Re
1200	$Co_{44}Nb_{21}Re_{35}$	50	χ-Re_3Nb/(εCo, Re)/λ_3	17.8	63.7	19.1	22.4	24.1	19.8
	$Co_{42}Nb_{34}Re_{24}$	50	μ-Co_7Nb_6/λ_3	34.9	27.0	33.0	20.5	…	…
	$Co_{25}Nb_{40}Re_{35}$	50	χ-Re_3Nb/bcc-(Nb)/μ-Co_7Nb_6	31.9	60.4	51.2	44.9	38.4	27.0
	$Co_{57}Nb_{21}Re_{22}$	50	(εCo, Re)/λ_3	18.0	28.8	22.3	17.8	…	…
	$Co_{44}Nb_{25}Re_{31}$	50	χ-Re_3Nb/λ_3	20.3	61.7	26.6	20.7	…	…
	$Co_{23}Nb_{49}Re_{28}$	50	bcc-(Nb)/μ-Co_7Nb_6	53.4	42.1	43.7	15.4	…	…
	$Co_{28}Nb_{50}Re_{22}$	50	bcc-(Nb)/μ-Co_7Nb_6	59.0	37.9	45.2	12.3	…	…
	$Co_{35}Nb_{30}Re_{35}$	50	χ-Re_3Nb/μ-Co_7Nb_6/λ_3	25.1	60.6	33.0	33.7	30.3	21.6
	$Co_{72}Nb_{18}Re_{10}$	35	λ_3/(αCo)	20.3	9.7	3.9	8.4	…	…
	$Co_{52}Nb_{39}Re_9$	35	μ-Co_7Nb_6/λ_3	43.4	9.3	34.9	7.8	…	…
	$Co_{23}Nb_{65}Re_{12}$	35	μ-Co_7Nb_6/bcc-(Nb)	52.4	2.8	78.8	19.4	…	…
	$Co_{64}Nb_{19}Re_{17}$	35	(εCo, Re)/λ_3	15.1	26.7	20.3	15.4	…	…
	$Co_{46}Nb_{37}Re_{17}$	35	μ-Co_7Nb_6/λ_3	39.8	17.4	34.5	15.5	…	…
	$Co_{23}Nb_{58}Re_{19}$	35	μ-Co_7Nb_6/bcc-(Nb)	50.1	6.5	66.9	30.1	…	…
	$Co_{47}Nb_{40}Re_{13}$	35	μ-Co_7Nb_6/λ_3	41.2	13.4	34.6	12.0	…	…
	$Co_{76}Nb_{13}Re_{11}$	35	λ_3/(αCo)	19.3	11.9	3.6	10.6	…	…
	$Co_{48}Nb_{33}Re_{19}$	35	λ_3	31.7	19.0	…	…	…	…
	$Co_{76}Nb_{20}Re_4$	35	λ_3/(αCo)	22.3	4.0	3.4	4.2	…	…
	$Co_{76}Nb_{18}Re_6$	35	λ_3/(αCo)	21.5	6.4	5.3	4.8	…	…
	$Co_{79}Nb_6Re_{15}$	35	(εCo, Re)/λ_3/(αCo)	2.9	17.2	19.3	13.2	3.1	12.2
	$Co_{71}Nb_{12}Re_{17}$	35	(εCo, Re)/λ_3	3.8	18.2	19.2	14.4	…	…
	$Co_{64}Nb_{25}Re_{11}$	35	λ_3	25.5	10.3	…	…	…	…
	$Co_{66}Nb_{29}Re_5$	35	λ_2	28.8	4.0	…	…	…	…
	$Co_{69}Nb_{29}Re_2$	35	λ_2	28.9	2.0	…	…	…	…
	$Co_{63}Nb_{23}Re_{14}$	35	λ_3	23.6	14.3	…	…	…	…
	$Co_{60}Nb_{35}Re_5$	35	λ_3	35.1	4.7	…	…	…	…
	$Co_{59}Nb_{40}Re_1$	35	μ-Co_7Nb_6/λ_3	47.3	1.3	36.4	1.0	…	…

Table 3 Equilibrium compositions of the Co-Nb-Re ternary system at 1300 °C determined in the present work

Temperature, °C	Alloy, at.%	Annealed time, days	Phase equilibria	Composition, at.%					
			Phase 1/Phase 2/Phase 3	Phase 1		Phase 2		Phase 3	
				Nb	Re	Nb	Re	Nb	Re
1300	$Co_{44}Nb_{21}Re_{35}$	25	χ-Re_3Nb/(εCo, Re)/λ_3	17.7	65.5	19.4	22.6	24.0	21.1
	$Co_{42}Nb_{34}Re_{24}$	25	μ-Co_7Nb_6/λ_3	34.4	27.7	33.1	20.4	…	…
	$Co_{25}Nb_{40}Re_{35}$	25	χ-Re_3Nb/bcc-(Nb)/μ-Co_7Nb_6	30.5	61.8	51.4	44.2	38.3	28.4
	$Co_{57}Nb_{21}Re_{22}$	25	(εCo, Re)/λ_3	18.4	29.4	22.1	19.0	…	…
	$Co_{44}Nb_{25}Re_{31}$	25	χ-Re_3Nb/λ_3	21.0	62.7	26.3	21.8	…	…
	$Co_{23}Nb_{49}Re_{28}$	25	bcc-(Nb)/μ-Co_7Nb_6	56.6	38.8	43.3	17.8	…	…
	$Co_{28}Nb_{50}Re_{22}$	25	bcc-(Nb)/μ-Co_7Nb_6	60.4	35.9	45.3	14.4	…	…
	$Co_{35}Nb_{30}Re_{35}$	25	χ-Re_3Nb/μ-Co_7Nb_6/λ_3	25.3	61.9	32.6	35.0	30.8	23.5
	$Co_{72}Nb_{18}Re_{10}$	15	λ_3/L	20.5	10.7	9.0	4.2	…	…
	$Co_{52}Nb_{39}Re_9$	15	μ-Co_7Nb_6/λ_3	43.3	9.8	35.9	8.2	…	…
	$Co_{23}Nb_{65}Re_{12}$	15	μ-Co_7Nb_6/bcc-(Nb)	51.3	3.6	77.8	19.2	…	…
	$Co_{64}Nb_{19}Re_{17}$	15	λ_3	20.2	16.0	…	…	…	…
	$Co_{46}Nb_{37}Re_{17}$	15	μ-Co_7Nb_6/λ_3	39.6	18.2	35.5	14.2	…	…
	$Co_{23}Nb_{58}Re_{19}$	15	μ-Co_7Nb_6/bcc-(Nb)	48.1	9.3	66.0	30.5	…	…
	$Co_{47}Nb_{40}Re_{13}$	15	μ-Co_7Nb_6/λ_3	41.4	14.3	35.2	11.8	…	…
	$Co_{76}Nb_{13}Re_{11}$	15	λ_3/(αCo)/L	19.7	13.0	4.4	11.9	6.4	4.1
	$Co_{48}Nb_{33}Re_{19}$	15	λ_3	32.3	19.0	…	…	…	…
	$Co_{76}Nb_{20}Re_4$	25	λ_3/L	22.8	4.5	13.1	2.0	…	…
	$Co_{76}Nb_{18}Re_6$	15	λ_3/L	21.5	7.4	11.7	3.4	…	…
	$Co_{79}Nb_6Re_{15}$	15	(εCo, Re)/λ_3/(αCo)	3.1	18.7	18.9	14.2	3.6	13.7
	$Co_{71}Nb_{12}Re_{17}$	15	(εCo, Re)/λ_3	4.1	19.1	18.9	14.9	…	…
	$Co_{64}Nb_{25}Re_{11}$	15	λ_3	25.7	10.2	…	…	…	…
	$Co_{66}Nb_{29}Re_5$	15	λ_2	30.0	4.0	…	…	…	…
	$Co_{69}Nb_{29}Re_2$	15	λ_2	28.9	1.8	…	…	…	…
	$Co_{63}Nb_{23}Re_{14}$	15	λ_3	23.9	14.1	…	…	…	…
	$Co_{60}Nb_{35}Re_5$	15	λ_3	35.5	4.8	…	…	…	…
	$Co_{59}Nb_{40}Re_1$	15	μ-Co_7Nb_6/λ_3	46.9	1.9	36.8	…		…

and $\lambda_3 + \lambda_2 +$ μ-Co_7Nb_6 at 1200 °C isothermal section, the former four three-phase equilibria were determined by $Co_{79}Nb_6Re_{15}$, $Co_{44}Nb_{21}Re_{35}$, $Co_{35}Nb_{30}Re_{35}$, and $Co_{25}Nb_{40}Re_{35}$ alloys, respectively. The last three-phase equilibrium was too small to be confirmed.

Figure 4(b) shows the isothermal section at 1300 °C of Co-Nb-Re system. Compared with the isothermal section of 1200 °C, the L phase appeared at Co-rich corner and dissolved about 4.1 at.% Re. And the L phase in our results was larger than that of the Co-Nb sub-binary system. As shown in Fig. 1, λ_1 phase existed in the sub-binary Co-Nb system at 1300 °C. But unfortunately, the λ_1 phase was not measured in this work. Thus, the singe λ_1 phase was plotted by dot line and two three-phase regions $\lambda_1 + \lambda_2 + \lambda_3$ and $\lambda_1 + \lambda_3 +$ μ-Co_7Nb_6 were predicted. It is worth mentioning that the λ_3 phase exists at the temperature range from 1029 to 1264 °C in the Co-Nb binary system, but it occurs as a stable phase at 1300 °C isothermal section in the Co-Nb-Re ternary system. The possible reason is that the λ_3 phase is stabilized to the higher temperature with the addition of element Re. The λ_3 phase appears at 1200 °C and it does not disappear at 1300 °C right now. The solubility of Re in the λ_3 phase was measured to be 23.8 at.%, a little larger than that in Fig. 4(a). The λ_2 phase dissolved about 5.6 at.% Re. The solubility of Re in the μ-Co_7Nb_6 phase was about 35.2 at.% and the solubility of Co in the χ-Re_3Nb phase was 16.9 at.%. The solubility of Nb in the (εCo, Re) phase was still large, about 18.8 at.%, which was almost the same as that at 1200 °C. The $Co_{64}Nb_{19}Re_{17}$ alloy located in the λ_3 single-phase region at 1300 °C, whereas it was a two-phase equilibrium at 1200 °C. Eight three-phase regions of (εCo, Re) + (αCo) + λ_3,

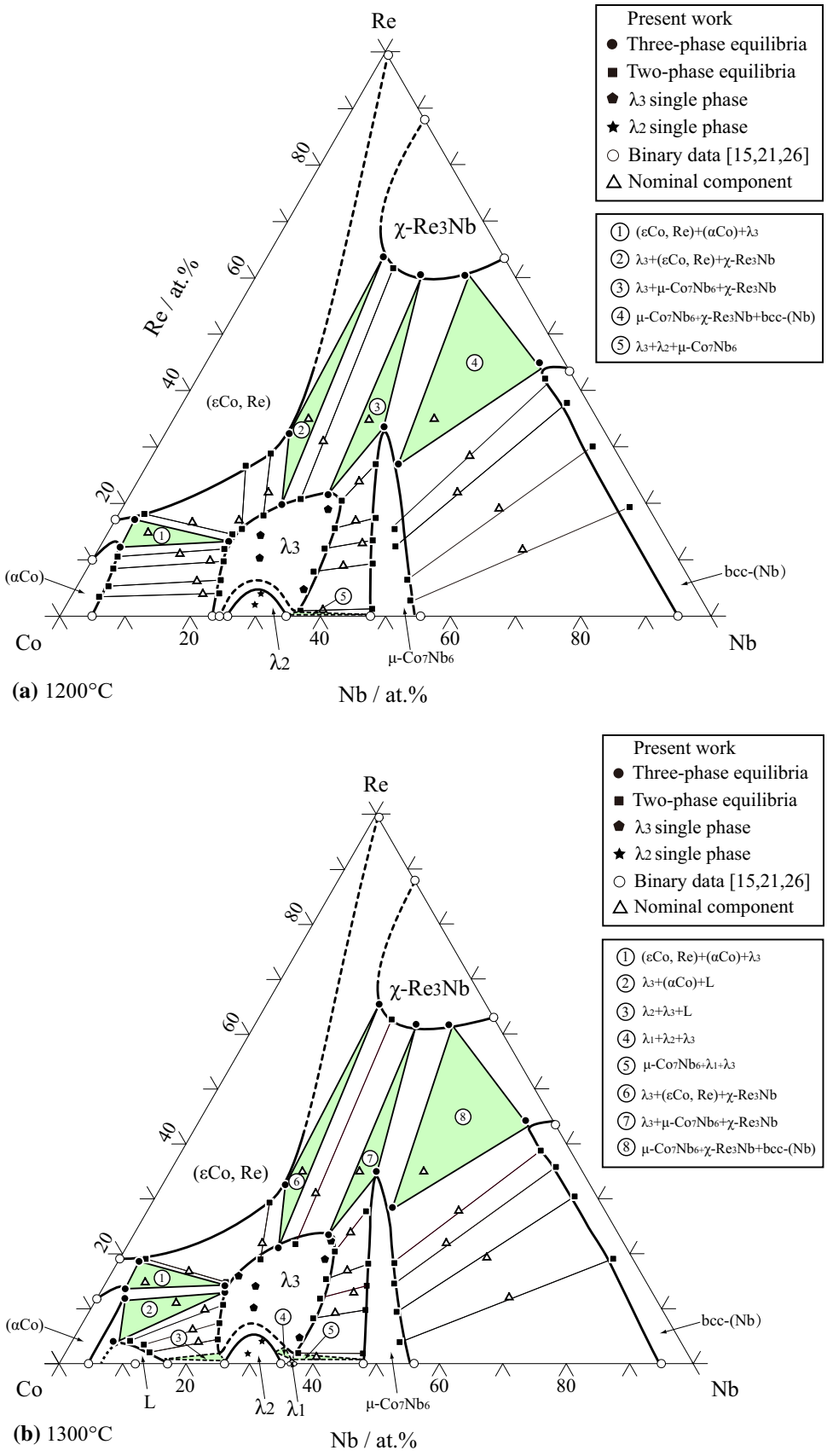

Fig. 4 Experimentally determined isothermal section of the Co-Nb-Re system: (a) 1200 °C, (b) 1300 °C

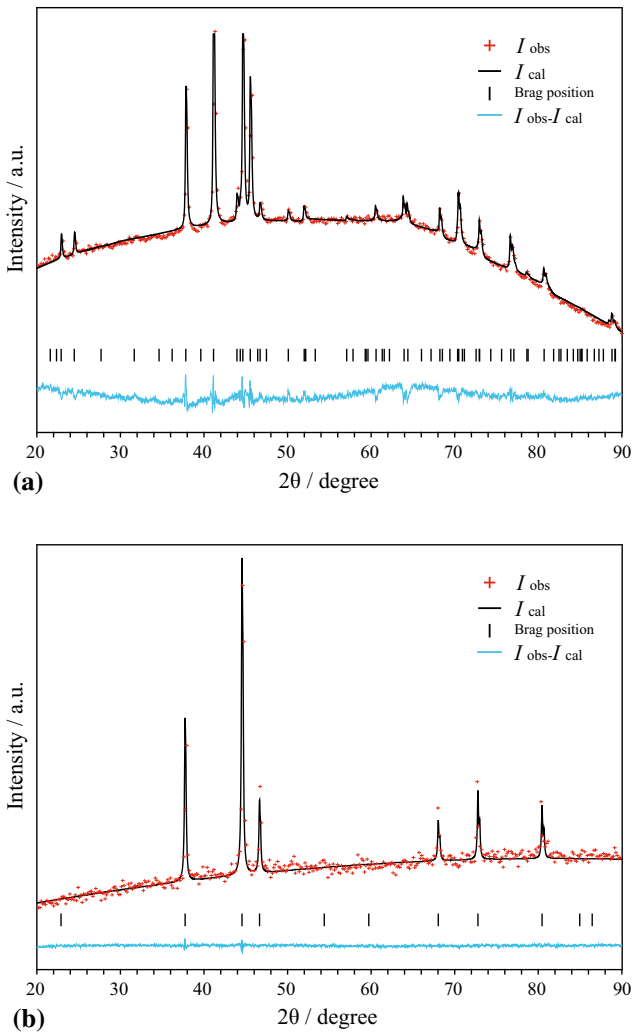

Fig. 5 Powder x-ray Rietveld refinement results (a) the $Co_{60}Nb_{35}Re_5$ alloy annealed at 1300 °C for 15 days; (b) the $Co_{66}Nb_{29}Re_5$ alloy annealed at 1300 °C for 15 days

λ_3 + (εCo, Re) + χ-Re_3Nb, λ_3 + μ-Co_7Nb_6 + χ-Re_3Nb, μ-Co_7Nb_6 + χ-Re_3Nb + bcc-(Nb), λ_3 + (αCo) + L, λ_2 + λ_3 + L, λ_1 + λ_2 + λ_3, and μ-Co_7Nb_6 + λ_1 + λ_3 existed in the isothermal section of 1300 °C. The former five three-phase regions were experimentally evidenced. The three-phase region of λ_3 + (αCo) + L occurred at 1300 °C, which is different with 1200 °C and the three-phase region of λ_3 + μ-Co_7Nb_6 + χ-Re_3Nb is a little smaller than that at 1200 °C.

Several single-phased alloys (λ_2, and λ_3) were prepared for further crystal structure analysis. Two representative crystal structures that refined by the Rietveld method for the $Co_{60}Nb_{35}Re_5$ and $Co_{66}Nb_{29}Re_5$ alloys are respectively shown in the Fig. 5(a) and (b). The experimental diffraction pattern (the red ticks) and the theoretical diffraction pattern (the black line) are presented below. The black vertical line presents the position of the Bragg peaks. The result gives a lattice parameter of a = 4.758(5) Å, and c = 15.527(2) Å for the λ_3 phase (space group: P63/mmc), and a lattice parameter of a = 6.747(4) Å for the λ_2 phase (space group: Fd-3 m).

4 Conclusions

Two isothermal sections at 1200 and 1300 °C of Co-Nb-Re ternary system were experimentally investigated. The results were concluded as following: (1) Five and eight three-phase regions respectively existed in the isothermal sections of 1200 and 1300 °C. (2) No ternary compound was found. (2) The Laves phase, λ_3 (C36), was stabilized to higher temperature of 1300 °C due to the Re addition. (3) The λ_3 phase had a large solubility of Re and wrapped around the λ_2 phase. (4) A small liquid region was confirmed at the isothermal section of 1300 °C but it was absent at the isothermal section of 1200 °C. (5) The composition range of (εCo, Re) was wide, extending from Co-rich side to Re-rich side. (6) The solubility of Re in the λ_2, λ_3, and μ-Co_7Nb_6 changed little from 1200 to 1300 °C.

Acknowledgments This work was supported by the National Key R&D Program of China (2017YFB0702901) and National Natural Science Foundation of China (51831007).

References

1. L.J. Shang, Q.K. Cai, C.S. Liu, and L. Qi, Effects of Re Doping on Properties of Co-Based Alloy Coating Treated by Laser Cladding, *Rare Met.*, 2002, **26**(3), p 173-178
2. Y.F. Cui, X. Zhang, G.L. Xu, W.J. Zhu, H.S. Liu, and Z.P. Jin, Thermodynamic Assessment of Co–Al–W System and Solidification of Co-Enriched Ternary Alloys, *J. Mater. Sci.*, 2011, **46**(8), p 2611-2621
3. D. Blavette, P. Caron, and T. Khan, An Atom Probe Investigation of the Role of Rhenium Additions in Improving Creep Resistance of Ni-Base Superalloys, *Scripta Metall.*, 1986, **20**(10), p 1395-1400
4. N. Wanderka and U. Glatzel, Chemical Composition Measurements of a Nickel-Base Superalloy by Atom Probe Field ion Microscopy, *Mater. Sci. Eng., A*, 1995, **203**(1), p 69-74
5. X.J. Liu, J.Y. Lin, Y. Lu, Y.H. Guo, and C.P. Wang, Assessment of the Atomic Mobility for the Fcc Phase of Ni–Co–X (X=Re and Ru) System, *CALPHAD*, 2014, **45**(3), p 138-144
6. E. Liu, X.R. Guan, and Z. Zheng, Effect of Rhenium on Solidification and Segregation of Nickel-Based Superalloy, *Rare Met.*, 2011, **30**, p 320-322
7. M. Huang and J. Zhu, An Overview of Rhenium Effect in Single-Crystal Superalloys, *Rare Met.*, 2016, **35**(2), p 127-139
8. A.C. Yeh, A. Sato, T. Kobayashi, and H. Harada, On the Creep and Phase Stability of Advanced Ni-Base Single Crystal Superalloys, *Mater. Sci. Eng. A*, 2008, **490**(1), p 445-451
9. A.F. Giamei and D.L. Anton, Rhenium Additions to a Ni-Base Superalloy: Effects on Microstructure, *Metall. Trans. A*, 1985, **16**(11), p 1997-2005

10. X.J. Liu, X.Q. Zhang, S.Y. Yang, C.C. Zhao, and C.P. Wang, Experimental Investigation of Phase Equilibria in the Co-W-Nb Ternary System, *Intermetallics*, 2012, **31**, p 48-54
11. J. Sha, H. Hirai, H. Ueno, T. Tabaru, A. Kitahara, and S. Hanada, Mechanical Properties of As-Cast and Directionally Solidified Nb-Mo-W-Ti-Si In-Situ Composites at High Temperatures, *Metall. Mater. Trans. A*, 2003, **34**(1), p 85-94
12. C.C. Shing, D.L. Douglass, and F. Gesmundo, The High-Temperature Corrosion Behavior of Co-Nb Alloys in Mixed-Gas Atmospheres, *Oxid. Met.*, 1992, **37**(3-4), p 167-187
13. R.P. Elliott, *Constitution of Binary Alloys*, First Supplement (McGraw-Hill Book Comp., New York, 1965)
14. B. Predel, Co-Re (Cobalt-Rhenium), *Ca-Cd-Co-Zr Springer Materials*, Vol 5C, O. Madelung, Ed., Springer, Berlin, 1993, p 1-3
15. C.P. Guo, T.F. Wu, C.R. Li, and Z.M. Du, Thermodynamic Re-Assessment of the Re–X (X=Al Co, Cr, Ta) Binary Systems, *CALPHAD*, 2018, **61**, p 33-40
16. J.K. Pargeter and W. Hume-Rothery, The Constitution of Niobium-Cobalt Alloys, *J. Less-Common Met.*, 1967, **12**(5), p 366-374
17. S.K. Bataleva, V.V. Kuprina, and V.Y. Markiv, Cobalt-Niobium Phase Diagram, *Moscow Univ. Chem. Bull.*, 1970, **25**, p 37-40
18. K.C. Hari Kumar, I. Ansara, P. Wollants, and L. Delaey, Thermodynamic Optimisation of the Co–Nb System, *J. Alloys Compd*, 1998, **267**(1), p 105-112
19. F. Stein, D. Jiang, M. Palm, G. Sauthoff, D. Grüner, and G. Kreiner, Experimental Reinvestigation of the Co–Nb Phase Diagram, *Intermetallics*, 2008, **16**(6), p 785-792
20. C.Y. He, F. Stein, M. Palm and D. Raabe, Thermodynamic Re-Assessment of the Co-Nb System. *MRS Proc*., 2008. https://doi.org/10.1557/PROC-1128-U05-30
21. C.Y. He, F. Stein, and M. Palm, Thermodynamic Description of the Systems Co–Nb, Al–Nb and Co–Al–Nb, *J. Alloys Compd.*, 2015, **637**, p 361-375
22. P. Greenfield and P.A. Beck, Intermediate Phases in Binary Systems of Certain Transition Elements, *JOM*, 1956, **8**(2), p 265-276
23. R. Steadman and P.M. Nuttall, Further Polymorphism in Cronstedtite, *Acta Crystallogr.*, 1964, **17**(4), p 404-406
24. A.G. Knapton, The Niobium-Rhenium System, *J. Less-Common Met.*, 1959, **1**(6), p 480-486
25. E.M. Savitskii, M.A. Tylkina, and K.B. Povarova, Phase Diagram for the Niobium-Rhenium System, *Sov. J. Atom Energy*, 1961, **7**(5), p 937-940
26. X.L. Liu, C.Z. Hargather, and Z.K. Liu, First-Principles Aided Thermodynamic Modeling of the Nb–Re System, *CALPHAD*, 2013, **41**(6), p 119-127